

MEMORANDUM FOR THE RECORD

SUBJECT: Comments on Value Function Analysis

1. This memorandum discusses four aspects of the application of the value function analysis approach to the OXCART/SR-71 comparison: i.e, the variation of "value" of stereo vs mono coverage, the effect of the atmosphere, "theoretical" versus "practical" approach, target contrast, and additive effects of multiple sensors.

2. Variation in value with resolution: In the current discussions, the "value" for resolutions below eight feet are given in tabular form; values at resolutions larger than eight feet are given by the formula $K(r) = 2.5/R$. However, the basic resolution variation with viewing angle is estimated as being proportional to the three halves power of the secant of the viewing angle. Unfortunately, such a combination yields an infinite area weighted value for 180° scan angle, as the area covered per unit angle is proportional to the secant squared. A value function of $20/R^2$ would remove this divergence, and yield a more realistic low value to large resolutions and match the proposed value at resolutions of about eight feet.

3. The "value" of Stereoscopic vs. monoscopic coverage: For some photo-interpretation and analysis tasks, stereoscopic coverage has some value; the value function thus should contain an explicit statement of the variation of values with stereo angle. I am not sure what this functional relationship should be for this mission (the value function chosen must, of course, be determined by the mission requirements).

4. The effect of atmospheric degradations: Many studies have shown that the resolution, for a given target contrast, is a function of the total haze contribution. Such total haze contribution (really the lowering of contrast of the target as presented to the camera) is affected by haze density, path length (hence obliquity), relative direction between sun-target ^{LINE} and camera-target line, etc. The currently accepted three halves power of secant of the viewing angle primarily reflects the increase of slant range and obliquity of horizontal targets. On the basis of the haze considerations, it is suggested that some higher power, say the square or five halves power, might be more appropriate, although this functional relation should be more carefully and explicitly considered.

5. Theoretical versus Practical Approach: Apparently the current approach to the value function analysis is to estimate ground resolution on the basis of a theoretical convolution of camera design parameters, vehicle motions, assumed accuracies, et cetera. I suggest that a more logical and pragmatic approach, in the case of operational cameras, is to use flight test results of nadir resolution. If desired, separate value functions could be derived for, say, the best, the average, and the worst, flight data, giving an expected spread in system value and concurrently, an estimate of the significance of difference in "value" for different systems.

6. Target Contrast: System resolution is directly related to target contrast; the contribution of haze, etc., is primarily in reduction of target contrast presented to the camera. Extreme care must be taken that, in studies and results applied, the contrast factors have been appropriately taken into account. For example, Air Force studies on haze problems assume a 9:1 contrast at the target; other aspects of performance may be based on 2:1 target at the camera, etc.

7. Additions of Values of Individual Sensors for a Multi-sensor System.

a. Case 1: Similar (e.g., two photo systems).

In this case we are considering the addition of value of, say, an extremely high resolution, narrow swath camera, and a moderate resolution, wide swath camera.

b. Case 2: Different sensors (e.g., a photo and an infra-red camera)

(to be determined)

8. Lineal versus Area Weighted Mission Value. The application of the value function analysis to satellite systems of long life and repetitive overflight of the same area had to consider film load limits and "non-duplicative" coverage. For the presently contemplated missions, neither the SR-71 nor the OXCART vehicle ^{is} are film limited, and the flight planner has a high degree of control over the flight path and coverage obtained. For these reasons, an adequate system value is

obtained, for comparison purposes, if one considers the lineal weighted value along a line perpendicular to the track of the aircraft, or for a short distance, say twenty to fifty miles, along the track. A further refinement, applicable to the Vietnam mission, would establish such a value for straight and level flight and another for banked flight; subsequently obtaining a weighted average based on an analysis of typical missions and the fraction of coverage normally obtained in banks.

cc: DP/SA
A/DD/S+T
DR. STEININGER
[redacted] NPIC
LES DIRKS/OSA

STAT

Value Function
Analysis.

The Probability Distribution of Camera Resolution

Milton D. Rosenau, Jr.

At each spatial frequency within a camera's resolution limit, the modulation of the camera exposure image will vary because of variation in object modulation, the atmosphere, the optical transfer function, and image motion. Thus, for each spatial frequency there is a probability that the image modulation will exceed that value required to resolve the image. This probability can be evaluated, even when the modulation detectability limit itself is variable. The resulting probability of resolution for each spatial frequency is directly observable in actual photographic results.

Introduction

The quality of a camera may be specified in terms of costs, cosmetic appearance, or other nontechnical aspects, but, to the technical worker, quality is usually synonymous with the ability of the camera to resolve detail, and to a lesser extent, with the field of view, focal length, etc. In the sense that quality is related solely to the actual resolution of detail, a considerable problem exists because the fact is frequently overlooked that quality varies from time to time and place to place in the same camera. The problem is of practical importance primarily in special purpose, servomechanically controlled cameras of high acuity such as ground-based telescopes and tracking cameras, and space-borne planetary reconnaissance cameras. In general, what follows concerns cameras with resolution of a few arc seconds or better, although much of what will be said has broader application.

Many descriptions, discussions, and specifications still use a single resolution value to characterize a camera despite evidence of the incompleteness of such characterization. In 1951, MacDonald¹ pointed out that there is a probability of detecting certain symbols, and, in 1953, in a discussion of how performance can be assessed, he presented data showing the frequency distribution of resolution for an aerial camera under certain conditions.² In 1954, Colwell³ discussed the probability of detection as related to photographic interpretation. But the fact that resolution should be expected to vary for reasons inherent in high-acuity photography has largely been ignored.

The quite satisfactory and generally widespread application of modulation transfer functions to describe

the photographic process now permits a rather simple and direct explanation of this quality variance. Further, as will be shown, the specific probability distribution to be expected of a particular camera can be calculated under certain conditions. Most importantly, this calculated distribution can be compared to directly observable resolution performance.

The most satisfactory basis for predicting and explaining the resolution limit of a camera is by the use of modulation transfer functions (MTF) to arrive at the exposure (or aerial) image modulation and to compare these values with modulation detectivity (as a function of spatial frequency) to ascertain the limiting resolution.⁴⁻⁶ The only restriction on this description of resolution limit is practical, in that a modulation detectivity curve must be constructed for the form of the resolution target and for the film-processing combination being employed.

Variations of Transfer Functions

Optical

The modulation transfer function of an optical system is the autocorrelation function of the pupil function, $G(x,y)$, where:

$$G(x,y) = e^{-(2\pi i/\lambda)\Delta(x,y)} \quad (1)$$

(x,y) is the coordinate of a point in the exit pupil, and $\Delta(x,y)$ is the optical path difference of the image-forming wavefront from an unaberrated spherical wavefront at (x,y) .

The lens designer generally assumes $\Delta(x,y)$ to be invariant in time, although recognizing that it may vary from one lens to another if several copies of the design are fabricated. Such variations are caused by homogeneity fluctuations in glass and by the fact that opticians cannot make lens surfaces perfectly or even

The author is with the Perkin-Elmer Corporation, Norwalk, Connecticut.

Received 9 August 1963.

identically on two supposedly identical lenses. The lens designer also recognizes that the modulation transfer function will be different at different field positions and focal planes because $\Delta(x,y)$ varies for these, and further, the modulation transfer function varies for different wavelengths. Thus, the basic lens cannot be described by a single modulation transfer function.

In practice, a further complication arises. The lens designer computes the required surface shapes on the assumption that a spherical wavefront emanates from the object and passes through the atmosphere (and, in some photography, a window) to impinge on the lens with a smooth shape, altered from spherical only, uniformly due, for instance, to postulated index gradients. However, atmospheric turbulence will distort the spherical (or, at least, smooth) wavefront and time-variant temperature nonuniformities in the glass (and window) will also distort the wavefront, so that $\Delta(x,y)$ can be expected to vary from time to time for the same lens in any one field and focal position at one wavelength.

Subject to certain restrictions, Hufnagel⁷ has calculated the average modulation transfer function of an unspherical optical wavefront with random wavefront variations. Thus, if we do calculate this average value and consider one field and focal position at one wavelength, the MTF, $T(k)$, is a single curve as shown in Fig. 1. For such a single-valued MTF, consider a particular spatial frequency k' ; the probability of $T(k')$ is unity, as shown in Fig. 2. (For simplicity, the MTF is treated as one-dimensional in this paper, but the extension to two dimensions is straightforward.)

However, even at this one field and focal position at one wavelength, the modulation transfer function is in actuality time variant, since the atmosphere is time variant.⁸ As a consequence, the MTF has a probability distribution, as shown in Fig. 3. The determination of the exact shape of such a probability distribution is difficult, but experiments may permit a satisfactory approximation.

The illustrated distribution is not Gaussian, since there is nothing known to suggest it should be, and the particular shape shown is not presumed to be a better estimate of what is correct. However, an upper limit to the modulation transfer function is set by the diffraction limit.

Obviously, the distribution will vary with spatial frequency and the other variables already discussed. Therefore, the size and nature of the sample of results being studied will also affect the observed distribution.

Image Motion

The MTF of image motion is also not a single fixed function. It varies with field angle, that is, from place to place in the focal plane, and it varies from time to

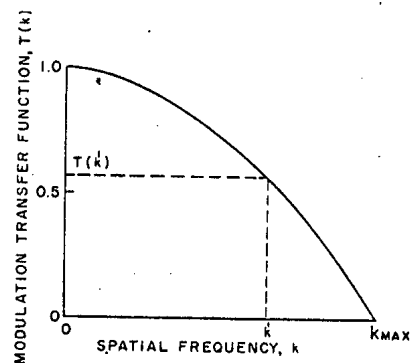


Fig. 1. Average modulation transfer function.

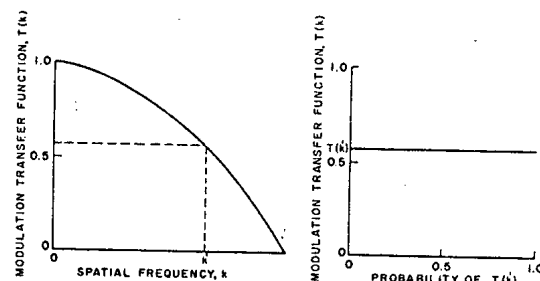


Fig. 2. Probability distribution of invariant MTF.

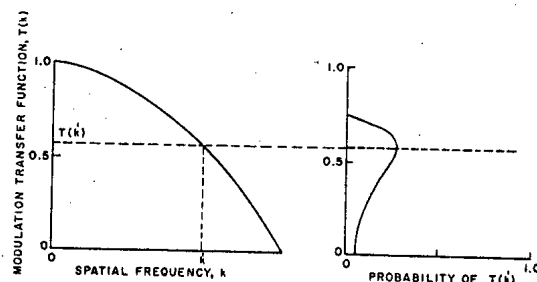


Fig. 3. Probability distribution of variable MTF.

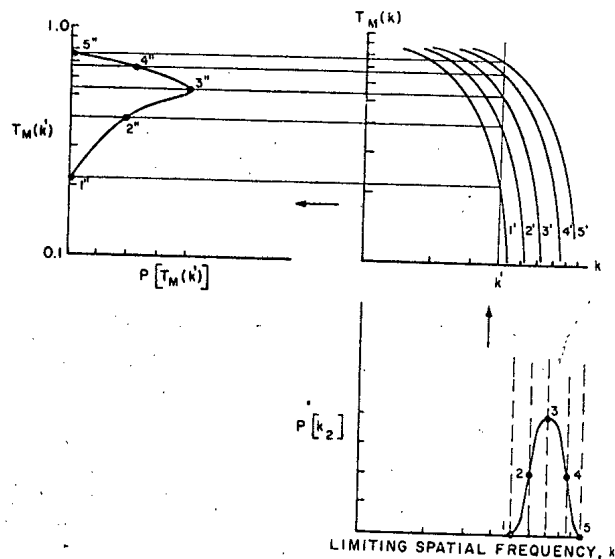


Fig. 4. Graphical estimate of the probability distribution of image motion MTF.

time at the same field position, but it is independent of focal plane (for distant objects) and wavelength.

As an obvious example of the dependence of the image motion MTF on field angle, consider the rotation of a camera about its optical axis. The axial image is unblurred, while points off the axis are blurred proportionally to the radius of the image from the axis in the sagittal direction and are unblurred in the tangential direction.

It is perhaps less obvious that the image motion MTF may vary from time to time at a single field angle. For instance, a stabilized camera is usually allowed a tolerable angular rate about each axis on the assumption that these combine as the square root of the sum of the squares. Thus, there are occasions of no angular velocity, tolerable angular velocity, excessive angular velocity, and, in fact, all rates up to that set by the sum of the actually achieved perfection of the hardware. Similarly, if sinusoidal vibration is present in the camera, the phase of the sinusoid at the initiation of exposure and the number of cycles occurring before the end of exposure affect the MTF profoundly.^{9,10} When several different kinds of image motion are present, the MTF is dependent on just how these image motions interact.

Consider the problem as it confronts the camera designer at the time mechanical tolerances must be established. As a specific example, say four mechanisms may produce image motion in one direction. The designer concludes that the magnitude of linear image motion which produces an acceptable modulation reduction is a , and he then assigns the four mechanisms $0.7a$, $0.5a$, $0.4a$, and $0.3a$, or some other distribution, such that the square root of the sum of the squares of the individual mechanism effects is equal to the tolerable total image motion. Now, even if these mechanisms turned out to be always as bad as the entire tolerance allowed and were random only in sign, then, for the specific example, the hardware would perform, within tolerance, about five-eighths of the time. An exact prediction of the resultant image motion obviously requires a detailed *a priori* knowledge of the way each mechanism will perform within the assigned tolerance. Thus, the camera designer will predict an image motion which is determined by the square root of the sum of the squares of the individual mechanism tolerances, and, generally, the camera will have less image motion than this value, but it may also occasionally have more.

The significant point is that the amount and type of image motion in a camera are not always the values predicted by the camera designer. As with the lens MTF, the image motion MTF has a probability distribution, the exact distribution depending on the sample considered.

Probability of Resolution

Simplified Case

To simplify the notion of probability of resolution, we temporarily restrict our attention to high-contrast objects of a form for which the modulation detectability curve is known, such as the USAF 1951 tri-bar pattern⁴⁻⁶; and we further assume that there is no scattering in the atmosphere to alter the apparent modulation.¹¹

Then we choose some spatial frequency, k' , at which the probability distributions of optical and image motion MTF's have been calculated. The probability distribution of the optical MTF, $P[T_o(k')]$, could be determined as follows: first, from optical design data or laboratory measurement, the MTF is determined at several field and focal positions; second, these are weighted by the expected frequency of occurrence; third, an estimated or experimentally determined adjustment is made for atmospheric turbulences; and fourth, these are combined to provide the probability distribution at each spatial frequency for which the optical transfer function has a particular value.

In the case of the probability distribution of the image motion MTF, $P[T_m(k')]$, this can be estimated in the camera design stage by estimating the probability of a certain magnitude of linear image motion. This estimate would result from a study of the tolerances of the camera's mechanisms and the interactions of these mechanisms. The easiest way to convert this to $P[T_m(k')]$ is graphically: first, the probability distribution of limiting spatial frequency is determined by taking the reciprocal of the image motion magnitude and weighting it appropriately; second, image motion MTF's are drawn for several cumulative percentages of occurrence, as in Fig. 4: and third, $P[T_m(k')]$ can be derived for each spatial frequency k' .

These two distributions, $P[T_o(k')]$ and $P[T_m(k')]$, respectively, are suitably combined* to arrive at the probability distribution of the system MTF (without film), $P[T_s(k')]$. In this simplified case, this is numerically equal to the probability distribution of modulation in the exposure image $P[M_E(k')]$. Since the film MTF can be placed in the modulation detectability function, this latter distribution determines the probability that the image at frequency k' will have sufficient modulation to be detected, as shown in Fig. 5. In this simplified case, the modulation detectability, $M_D(k')$, is assumed invariant. The probability distributions are presumed to be suitably normalized.

Similar determinations are made at other spatial frequencies, and the result, the probability of resolving

* A method similar to that discussed in the Appendix, in which equal probability "bands" are suitably multiplied, is probably adequate. For a rigorous mathematical method see, for instance, J. S. Bendat, *Principles and Applications of Random Noise Theory* (Wiley, New York, 1958), pp. 105-124.

each frequency, can be related to the frequency, as shown in Fig. 6.

General Case

In the general case, the modulation reduction due to scattering, ϕ , has a probability distribution,¹¹ $P[\phi]$. Since ϕ is independent of spatial frequency, so is $P[\phi]$. Again, the exact nature of this distribution depends on the sample of photography considered, since ϕ depends on the length and orientation of the air column through which the photograph is taken, the condition of the atmosphere, and brightness. Except for very short air columns, ϕ is considerably less than 1.0, and $\phi = 0.8$ seems to be a maximum value for practical conditions when photographing through the complete atmosphere under the clearest observed conditions.

Since $\phi < 1$ simply lowers the modulation in the exposure (or aerial) image, $P[\phi]$ can be combined with $P[T_s(k')]$ to obtain a probability distribution of the exposure image modulation, $P[M_E(k')]$ which is a function of spatial frequency, k' , because $P[T_s(k')]$ is a function of spatial frequency.

Similarly, object modulation, M_o , may be less than 1.0, and this too will have a probability distribution. In some cases, this distribution will be dependent on the spatial frequency of the object,¹² and for complete generality, we characterize this object modulation probability distribution as $P[M_o(k')]$.

Now, it is clear that the general statement of the probability distribution for exposure (or aerial) image modulation is

$$P[M_E(k')] = \{P[M_o(k')]\} \{P[\phi]\} \{P[T_o(k')]\} \{P[T_M(k')]\} \quad (2)$$

where the right-hand side of the equation is understood to be an appropriate combination in which modulations and transfer functions are multiplied. This complete probability distribution must be evaluated at each frequency k' of interest to determine the probability of the exposure modulation exceeding that required for resolution, as given by the modulation detectability curve. The final result is graphed as in Fig. 6. Alternatively, $P[M_o(k')]$ can be omitted from $P[M_E(k')]$ and separate curves, like those in Fig. 6, can be drawn for several values of M_o .

The evaluation of the probability that the exposure image modulation exceeds that required by the modulation detectability limit is more complicated when the modulation detectability limit is also variable as when granularity fluctuations are integrated over only small target images or when processing variations are significant. In such a case, the probability distribution of the modulation detectability, $P[M_D(k')]$, will be a function of spatial frequency.

Extending the method illustrated in Fig. 5, the probability of resolving an image at frequency k' is:

$$\int_0^1 P[M_D(k')] \left\{ \int_{M_D}^1 P[M_E(k')] dM_E \right\} dM_D. \quad (3)$$

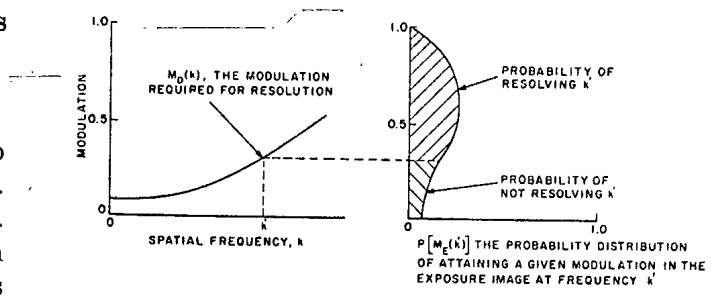


Fig. 5. Probability of resolving frequency k' .

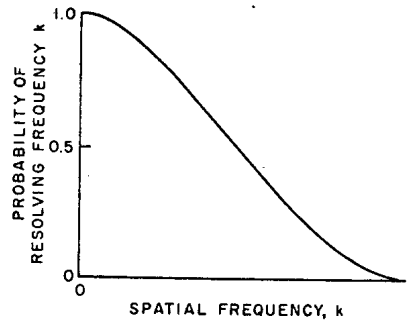


Fig. 6. Probability distribution of resolution.

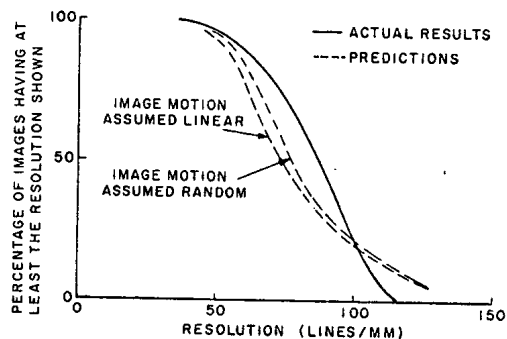


Fig. 7. Actual and predicted results.

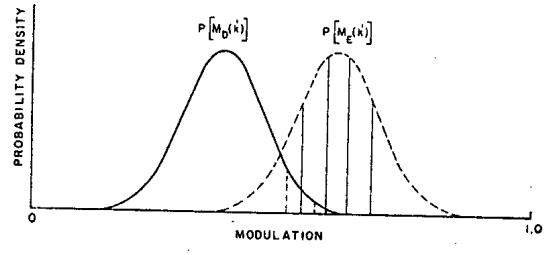


Fig. 8. Graphical evaluation of Eq. (3).

As a practical matter, this can be approximately evaluated graphically or in the form

$$\sum_{i=1}^{i=n} P_i[M_D(k')] \left\{ \int_{M_D}^1 P[M_E(k')] dM_E \right\}, \quad (4)$$

where n is a small number (e.g., 3, 4, or 5) and M_D is the average value of modulation detectability in a region n^{-1} of the distribution. (See Appendix.)

Other Variables

In the discussion so far, it has been presumed that the many other variables affecting photographic quality are under good control. This is not unreasonable for a wide variety of practical situations. However, it must be recognized that many variables (e.g., exposure, specular reflections, atmospheric absorption, spectral sensitivity, degree of polarization, processing, etc.) affect the quality of the final image. If any of these other variables have an influence which is substantial compared with those previously considered, then suitable probability distributions for these must also be included in the analysis.

Experimental Example

Brown¹³ provided data from laboratory tests of a camera which showed the kind of probability distribution illustrated in Fig. 6. This is shown in Fig. 7. Also shown in Fig. 7 are two *a posteriori* predictions of the actual results. The actual result is in reasonable agreement with both predictions; whether the difference in prediction and actual result is significant would depend on the application.

The actual result was obtained with a USAF 1951 high-contrast tri-bar target projected into the camera under test from a laboratory collimator; 140 images were obtained from a total of twelve different test conditions. Only axial images were obtained. Kodak SO-130 film developed in D-19 for 8 min was used. The 140 images provided 280 radial and tangential resolution readings, which were made through a binocular microscope. Table I contains the raw data.

The two predictions were made from theoretical lens and film data, and the image motion was estimated from other laboratory tests of the camera performed with Kodak SO-102 film. These other laboratory tests were performed under the same twelve conditions, but the number of images obtained in each condition differed, and only 113 images were obtained, so these results were weighted by the ratio of images with SO-130

to images with SO-102. Table II contains the raw data from SO-102.

To obtain an "effective" modulation detectability curve, the MTF of the film and lens were added into the modulation detectability function, $M_D(k)$, as given for SO-102.⁴ An ogive of linear image motion limiting frequency and also of random image motion limiting frequency was derived so as to satisfy the weighted results obtained on SO-102 film. The intersection of linear and random image motion MTF's with an "effective" modulation detectability function for SO-130 produced the two predicted results shown in Fig. 7, where the percentages are those from the ogives obtained from SO-102. (The constant, 0.04, used in the modulation detectability function with SO-102 film was replaced by 0.03 for SO-103 film.¹⁴) Since the probability distribution of modulation detectability was felt to be very small compared to the image motion variability, a single value of detectability was used at each frequency.

No plausible explanation has so far been found to improve the agreement of prediction and results shown in Fig. 7. Differences in image motion between the test with SO-102 and SO-130 are most likely, but incorrect assumptions regarding the optical transfer function, the modulation detectability for the films, and the variability of exposure and processing are also quite possible.

Conclusions

A logical approach and physical basis to account for and predict the probability distribution of camera resolution has been proposed. The distribution curve obtainable from *a priori* prediction (Fig. 6) is an observable function, and, therefore, an experimental verification is possible. Specifically, the percentage of images resolving a higher frequency than each spatial frequency k' can be determined by inspecting actual photographic results. If the sample of actual photography was obtained under the conditions on which the analytic pre-

Table I. Number of Images Having Given Resolution. SO-130 Test Data

Test condition	Resolution (L/MM)														
	128	114	102	91	81	72	64	57	51	46	41	37	33	29	
1			4	7	4	1									
2			2	12	11	5	3	1							
3			1	3	3	1	2	1	3		2				
4				2	4	3	1		2						
5			1	6	13	16	6		1				1		
6			2	1	1		2	7	2	1					
7	1		15	3		3									
8			3	13	6	4	1	1	1	1	1				1
9			1	2	1	3	2	3	2	2	1	1			
10				7	4	5									
11		3	12	7	5	8		1							
12			2	4	3	3	3	2					1		

Table II. Number of Images Having Given Resolution. SO-102 Test Data

Test condition	Resolution (L/MM)										
	91	81	72	64	57	51	46	41	37	33	29
1		3	4	1	2						
2			3	10	9	13			1		
3				1	1	6					
4			1	3	4	2	4				
5			1		12	6	7	5	6	1	
6				2	1	3	1		2	1	
7	1	4	4	2	1						
8		6	11	11	9	2			3		
9	1	1	3	1	2						
10		4	4	2		1		1			
11	1	5	5	7	9	7	1		1		
12			2	1	2	3	1				1

dictions were made, the percentage of images resolving more than each frequency k' should be identical with a prediction curve like Fig. 6. An experimental example shows a reasonable agreement of prediction and result.

Finally, it should be evident that discussions of a resolution limit of a camera must be qualified by the frequency of attainment which is intended.

The data used in the example resulted from work being carried out by E. B. Brown and were called to our attention by him. It is also a pleasure to acknowledge helpful discussion with R. C. Babish, R. E. Hufnagel, H. D. Polster, F. Scott, R. M. Scott, and R. V. Shack.

Appendix

Graphical Evaluation of Eq. (3)

Equation (3) evaluates the probability that the exposure image modulation exceeds the modulation detectability limit, where both modulations are variable and described by probability distributions. In Fig. 8 a hypothetical case is illustrated for a single spatial frequency. The probability distribution for the exposure image modulation is divided into five bands, each representing 20% total probability. The midpoint modulation of each band is located and the cumulative

percentage of the modulation detectability which falls below this value is noted. This is repeated for each of the five 20% bands. In the illustrated case, where Gaussian probability distributions are used, the probability of resolution would be estimated as:

$$0.2 \times 0.94 + 0.2 \times 0.98 + 0.2 \times 0.996 + 2 \times 0.2 \times 1.0 = 0.98.$$

References

1. D. E. MacDonald, "Optical Image Evaluation", NBS Circular 526, 51ff (1951).
2. D. E. MacDonald, *J. Opt. Soc. Am.* 43, 290 (1953).
3. R. N. Colwell, *Photogram. Eng.* 20, 433 (1954).
4. *The Practical Application of Modulation Transfer Functions*, (Perkin-Elmer Corporation, Norwalk, Connecticut, 1963), chap. 4.
5. G. C. Brock, W. L. Attaya, and E. P. Myskowski, "Study of Image-Evaluation Techniques", Itek Report 9048-1 (1962), Astia Doc. No. AD286488.
6. C. E. Campbell, *Photogram. Eng.* 28, 446 (1962).
7. Reference 4, chap. 3.
8. E. Djurle and A. Back, *J. Opt. Soc. Am.* 51, 1029 (1961).
9. "A Scientific Investigation into Photographic Reconnaissance from Space Vehicles", Cornell Aero. Lab. Report No. VF-1260-P-2 (1959), Astia Doc. No. 289667.
10. R. V. Shack, "The Influence of Image Motion and Shutter Operation on the Photographic Transfer Function" (to be published).
11. M. D. Rosenau, *Phot. Sci. Eng.* 6, 265 (1962).
12. Reference 4, chap. 1.
13. E. B. Brown, private communication (April 1963).
14. R. E. Hufnagel, private communication (June 1963).



George C. Higgins *Eastman Kodak*, (left) Editor for this issue's feature on Optics of the Photographic System, and W. Lewis Hyde *Institute of Optics*.